AGU PUBLICATIONS

Earth and Space Science

RESEARCH ARTICLE
10.1002/2016EA000199

Key Points:
- A model-observation discrepancy in the tropical O_3 response to the 11 year solar cycle persists for more than 20 years
- An artificial O_3 decadal variability caused by orbital drifts has been misidentified as the 11 year solar modulation
- If the orbital drifts are well considered, then the 11 year solar cycle response in O_3 is consistent with model predictions

Correspondence to:
K.-F. Li,
kfli@uw.edu

Citation:
Li, K.-F., Q. Zhang, K.-K. Tung, and Y. L. Yung (2016), Resolving a long-standing model-observation discrepancy on ozone solar cycle response, *Earth and Space Science*, *3*, 431–440, doi:10.1002/2016EA000199.

Received 27 JUL 2016
Accepted 3 OCT 2016
Accepted article online 8 OCT 2016
Published online 28 OCT 2016

©2016. The Authors.
This is an open access article under the terms of the Creative Commons Attribution-NonCommercial-NoDerivs License, which permits use and distribution in any medium, provided the original work is properly cited, the use is non-commercial and no modifications or adaptations are made.

Resolving a long-standing model-observation discrepancy on ozone solar cycle response

King-Fai Li[1], Qiong Zhang[2], Ka-Kit Tung[1], and Yuk L. Yung[2]

[1]Department of Applied Mathematics, University of Washington, Seattle, Washington, USA, [2]Divisions of Geological and Planetary Sciences, California Institute of Technology, Pasadena, California, USA

Abstract To have the capability for long-term prediction of stratospheric ozone (O_3), chemistry-climate models have often been tested against observations on decadal timescales. A model-observation discrepancy in the tropical O_3 response to the 11 year solar cycle, first noted in 1993, persists for more than 20 years: While standard photochemical models predict a single-peak response in the stratosphere, satellite observations show an unexpected double-peak structure. Such discrepancy has led to the question of whether the current standard O_3 photochemistry is deficient. Various studies have explored uncertainties in photochemistry and dynamics but there has not been compelling evidence of model biases. Here we suggest that decadal satellite orbital drifts relative to the diurnal cycle could be the primary cause of the discrepancy. We show that the double-peak structure can be reproduced by adding the A.M./P.M. diurnal difference to the single-peak response predicted by the standard photochemistry. Thus we argue that the standard photochemistry is consistent with the observed solar cycle modulation in stratospheric O_3.

1. Introduction

Ozone plays a fundamental role in the Earth's atmosphere. Produced by the absorption of UV light, the ozone layer shields the surface of the planet from damaging UV radiation, allowing the development of an advanced biosphere and eventually intelligent life. Ozone is also a key molecule in the energy budget of the atmosphere. The ozone layer is primarily responsible for the dramatic temperature inversion above the tropopause; absorption by the Chappuis band in the visible wavelength region contributes to heating of the troposphere. Due to its strong absorption in a band at 9.6 μm, ozone is the third most important greenhouse molecule on this planet after H_2O and CO_2. As emissions of halocarbon have been regulated since the 1990s, recovery of stratospheric O_3 helps cool the surface by reducing downwelling shortwave radiation in the upper stratosphere while also strengthens greenhouse warming by enhancing the absorption of outgoing longwave radiation in the lower stratosphere. The net effect of these two large canceling terms is sensitive to the vertical structure of stratospheric O_3 [*Forster and Shine*, 1997]. The latest Intergovernmental Panel for Climate Change assessment (AR5) reports that the radiative forcing of stratospheric O_3 in 16 chemistry-climate models ranges widely from -0.15 to $+0.05\,W\,m^{-2}$, due largely to the different vertical structures of ozone in the models [*Myhre et al.*, 2013]. Therefore, it is important that models' vertical structure be validated against observation. It then follows that our understanding of ozone photochemistry may be in serious doubt if the models cannot reproduce the observed vertical structure of ozone.

Indeed, the theory of stratospheric O_3 has been revised a number of times since its discovery in the nineteenth century. The first photochemical model was proposed by Sydney Chapman in 1930, in which the ultimate source of stratospheric O_3 is the photodissociation of molecular oxygen (O_2) by solar UV below 240 nm into atomic oxygen (O), followed by the recombination of O with O_2 to form O_3; O_3 is lost primarily through either photodissociation at 200–360 nm or recombination with O [*Chapman*, 1930]. However, the Chapman chemistry alone overestimates stratospheric O_3, prompting the introduction of catalytic depletion by hydrogen oxides and nitrogen oxides in the 1950s and 1960s [*Bates and Nicolet*, 1950; *Crutzen*, 1970]. The discovery of the Antarctic O_3 hole in 1985 further stimulated proposals on polar-night stratospheric dynamics and new catalytic depletion by bromine oxides, but it is the chlorine radicals released from man-made chlorofluorocarbons that cause the severe heterogeneous catalytic O_3 depletion [*Yung et al.*, 1980; *Farman et al.*, 1985; *McElroy et al.*, 1986; *Solomon et al.*, 1986; *Tung et al.*, 1986; *Molina and Molina*, 1987; *Sander et al.*, 1989].

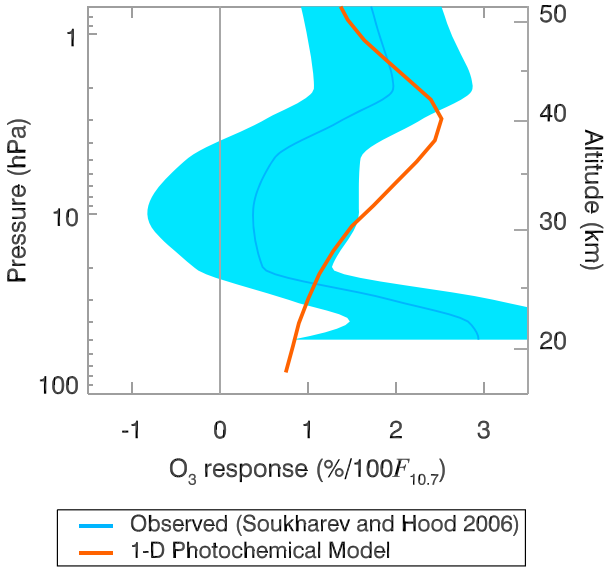

Figure 1. The double-peak structure of 11 year solar cycle response in the stratospheric ozone reported in *Soukharev and Hood* [2006] (blue line), based on Figure 4 of *Austin et al.* [2008]. The error of the observed response (cyan shade) represents 2σ levels. For comparison, a single-peaked response simulated using the 1-D Caltech/JPL photochemical model is also shown (orange line).

Global O_3 distribution is also determined by the meridional residual (Brewer-Dobson) circulation, especially in the lower stratosphere, which transports O_3 from low latitudes (where it is photochemically produced) to high latitudes [*Brewer*, 1949; *Dobson*, 1956]. More details of O_3 photochemistry and transport can be found in standard text books, e.g., *Yung and DeMore* [1999] and *Brasseur and Solomon* [2005].

The Chapman chemistry together with catalytic and heterogeneous reactions now forms the standard photochemistry of O_3. Thus far, this standard model of O_3 has been successful in predicting short-term (e.g., diurnal to annual) variability of stratospheric O_3. However, to monitor O_3 changes on longer timescales that are relevant to O_3 recovery and climate change, the standard model must be validated against long-term observations. The 11 year solar cycle has often been used for this purpose, as this natural phenomenon has a well-measured quasiperiodic radiative source. (Due to the calibration of different satellites, there is uncertainty in the satellite-measured absolute value of the solar constant, but the impact on this relative oscillation is minor [*Solanki et al.*, 2013].) Variations in solar UV affect both the photochemical production and destruction of O_3. The 11 year solar cycle modulation in O_3 was first studied by *Willett* [1962] using total column O_3, but the modulation in the vertical O_3 profile was not revealed until satellite data became available in the 1970s. With the standard photochemistry, the vertical O_3 response to the 11 year solar cycle in the tropical upper stratosphere is governed primarily by the Chapman chemistry and is a single-peak structure with a peak response at 3 hPa of ~2.5% per 100 units of 10.7 cm solar radio flux (%/100 $F_{10.7}$). However, the observed response is significantly different. Using the 11.5 years of O_3 data from National Aeronautics and Space Administration (NASA) Solar Backscatter Ultraviolet measurement (SBUV) since 1979, *Hood et al.* [1993] derived a vertical O_3 response that featured the so-called "double-peak" structure (Figure 1): there are statistically significant positive responses in the upper stratosphere (~2%/100 $F_{10.7}$) at 40–55 km (0.3–3 hPa) and the lower stratosphere (~3%/100 $F_{10.7}$ near 20 km or 100 hPa) while the response in the middle stratosphere (30–40 km or 3–30 hPa) is practically zero. The double-peak structure persisted when longer SBUV O_3 records (version 8) were included [*Soukharev and Hood*, 2006].

The observed double-peak structure poses a number of challenges to the standard photochemistry. We shall examine these challenges in more details in section 3.3, but we briefly summarize them here. First, the upper stratospheric peak is located at a higher altitude than predicted (~35 km) by photochemical production of O_3 [*Brasseur et al.*, 1988; *Austin et al.*, 2008]; there has not been any attempt to explain the shift in the upper stratospheric peak. Second, many modeling studies attempt to explain the weak middle stratospheric response in terms of solar-induced effects on stratospheric dynamical processes, such as the quasi-biennial oscillation (QBO) [*Smith and Matthes*, 2008; *Matthes et al.*, 2013] and the Brewer-Dobson circulation, or more realistic dynamical fields from reanalyses [*Dhomse et al.*, 2011]. Potential effects due to solar-induced changes in ozone-destroying catalysts, such as the odd-nitrogen species, and modeling errors due to observational uncertainties in the solar UV variability have also been studied extensively [*Rozanov et al.*, 2005; *Haigh et al.*, 2010; *Ball et al.*, 2014a, 2016]. While some of these attempts managed to simulate a weaker middle stratospheric response than suggested by the standard chemistry [*Austin et al.*, 2008; *Dhomse et al.*, 2011; *Chiodo et al.*, 2012], the simulated response is still robustly positive rather than being nearly zero as observed. Lastly, the lower stratospheric maximum, which occurs at an altitude where photochemistry is not dominant, has

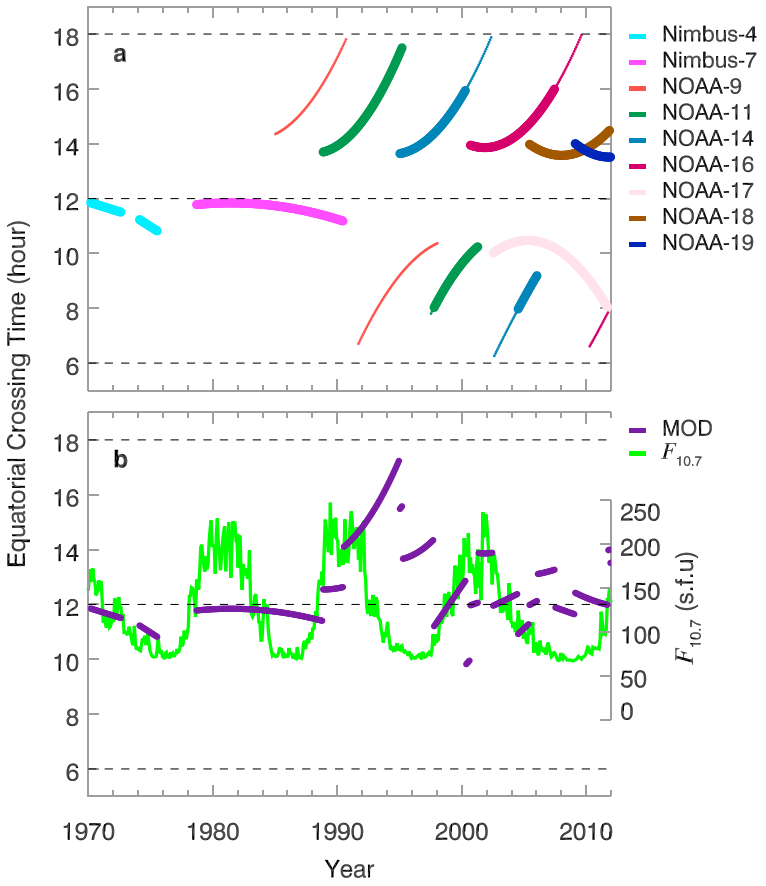

Figure 2. (a) The equatorial crossing times (ECT) of individual satellite platforms that carried the SBUV instruments. Thick lines represent measurements that are included in the MOD products. In the MOD products, all data (except NOAA-11) with ECT before 8 A.M. and after 4 P.M. are excluded (represented by thin lines). These ECT data are extracted from *Bhartia et al.* [2013]. (b) The "estimated" average ECT corresponding to the MOD products, based on the assumption that the O_3 concentrations in the overlapping periods are simple arithmetic averages of individual measurements. For comparison, the 10.7 cm solar radio flux ($F_{10.7}$) is also shown.

been attributed to the influence of the El Niño–Southern Oscillation (ENSO) or aliasing with major volcanic eruptions in 1983 (El Chichón) and 1992 (Pinatubo) that were almost a decade apart, although some studies question the robustness of these effects [*Marsh and Garcia*, 2007; *Hood and Soukharev*, 2012; *Chiodo et al.*, 2014; *Dhomse et al.*, 2015].

To date, the above proposed solutions have approached the double-peak structure problem mainly from modeling perspectives; none focused on the O_3 data itself. Here we argue that while we must understand the physical processes, accurate knowledge of how data were acquired is also critical when interpreting the observed variability. We propose a possible resolution for this model-observation discrepancy in the O_3 decadal variability, namely, the diurnal bias of data acquisition due to orbital drifts. Section 2 reviews the decadal variability of the orbits carrying the SBUV instruments. Section 3 describes the methodology used to calculate the decadal effects on O_3. Section 4 discusses the results and their implications.

2. Data and Methods

The SBUV data are publicly available on the World Wide Web (http://acd-ext.gsfc.nasa.gov/Data_services/merged/). The SBUV instruments were launched into drifting orbits, where overpassing time varies over the course of the mission [*DeLand et al.*, 2012]. Figure 2a shows the equatorial crossing times (ECTs) of the SBUV carriers since 1970. Except for Nimbus-4 and Nimbus-7, which had relatively stable orbits, all NOAA platforms experienced orbital drifts a few years after launch. As a result, SBUV O_3 measurements are subject to large diurnal variations since the time of the day when measurements were taken drifted. As illustrated in

Figure 14 of *Bhartia et al*. [2013], which shows the ratio of the NOAA-17 and NOAA-18 measurements corresponding to 10 A.M. and 2 P.M., respectively, O_3 is more abundant in the afternoon at altitudes above 5 hPa or below 30 hPa and is less abundant between 5 and 30 hPa; the lower stratospheric diurnal variability is due to dynamics [*Haefele et al*., 2008]. This vertical structure of the A.M./P.M. asymmetry thus exhibits a double-peak profile that is similar to that of the "observed" O_3 solar cycle response.

If the A.M. and P.M. measurements are randomly distributed over the solar cycle phases, then the A.M./P.M. asymmetry may cancel each other in the linear regression. However, Figure 2b shows that this is true only before 1990 or after 2000. During the solar minimum period 1990–2000, there were more P.M. than A.M. measurements. The average ECT over this period is 2 P.M. while $F_{10.7}$ is -50 solar flux unit ($1\ \text{sfu} = 10^{-22}\ \text{W m}^{-2}\ \text{Hz}^{-1}$) relative to the mean value. Linear regression applied to the whole O_3 record, e.g., over 1979–2004, as in *Soukharev and Hood* [2006], might misidentify the A.M./P.M. asymmetry in 1990–2000 as a solar minimum response. We explore this possibility using the Caltech/Jet Propulsion Laboratory (JPL) 1-D photochemical model [*Allen et al*., 1981, 1984] to simulate the effect of the diurnal bias to the O_3 decadal variability. This model contains 66 levels from the surface to 130 km altitude. Vertical transport is parameterized using eddy diffusion. The chemical kinetics is based on the JPL's Chemical Kinetics Evaluation in 2006 [*Sander et al*., 2006]. The model contains 12 atoms, 617 molecules, and 2248 reactions. The important species involved in this work include: O, $O(^1D)$, O_2, $O_2(^{1/\Delta})$, O_3, NO, NO_2, N_2O, HNO_3, H, OH, H_2, H_2O, and H_2O_2. The model is run until photochemical equilibrium is reached. Then the vertical O_3 profile at the photochemical equilibrium is examined.

While the 1-D photochemical model provides a simple way to illustrate the solar cycle modulation on O_3, photochemistry dominates only above the middle stratosphere. Meriodional transport, which is important in the lower stratosphere, is absent in the model. Furthermore, there is no aerosol injection from the tropical troposphere into the stratosphere in the model. Missing these two factors means that the 1-D model will not be capable of simulating the aliasing between the volcanic eruptions and the 11 year solar cycle. *Chiodo et al*. [2014] showed using a 3-D model that such aliasing is largely responsible for the presence of the lower stratospheric peak, suggesting that the lower peak is not related to the solar forcing. We will use their simulation to reconstruct the observed O_3 solar cycle response in section 3.1.

A solar UV flux input is required for photochemical processes. For wavelengths between 115 and 400 nm, we use the mean solar spectral UV in 2004 (neutral solar cycle conditions) measured by the National Aeronautics and Space Administration (NASA)'s Solar Radiation and Climate Experiment (SORCE). There are two instruments aboard SORCE. The first instrument, Solar Stellar Irradiance Comparison Experiment (SOLSTICE), measures the UV intensity for wavelengths between 115 and 340 nm and has better performance on short wavelengths; we use the SOLSTICE data for wavelengths $\leq$240 nm. The other instrument, Spectral Irradiance Monitor (SIM), measures the spectral intensity for wavelengths between 200 and 2400 nm and has better performance for long wavelengths; we use the SIM data for wavelengths $\geq$240 nm.

The solar UV spectral variability over the 11 year solar cycle is based on the Naval Research Laboratory's solar spectral irradiance model [*Lean*, 2000]. It attains the largest variability (15%) at the Lyman-α emission line (121.57 nm) and drops to nearly zero at 300 nm. Detailed variations of the spectral irradiance over a typical 11 year solar cycle can be found in Figure 3 of *Wang et al*. [2013]. We use this spectral model to drive the solar cycle variability in the photochemistry.

3. Results and Discussions

3.1. Simulated Effects of Orbit Drifts

We perform two experiments using the 1-D photochemical model. The first experiment (Experiment A) is to calculate the response of O_3 to spectral UV changes corresponding to $\Delta F_{10.7} = -50$ sfu, which represents the solar cycle modulation. The result is shown as the dashed line in Figure 3. This profile is the equivalent to the one shown in Figure 1, up to a scaling factor that accounts for different values of $\Delta F_{10.7}$. As discussed in section 1, this photochemical O_3 response to the 11 year cycle is dominated by a single peak ($1.5\%/100\ F_{10.7}$) at 3 hPa in the upper stratosphere due to the Chapman chemistry. The second experiment (Experiment B) is to calculate the O_3 diurnal change at 2 P.M. relative to 12 P.M., which represents the A.M./P.M. diurnal asymmetry due to

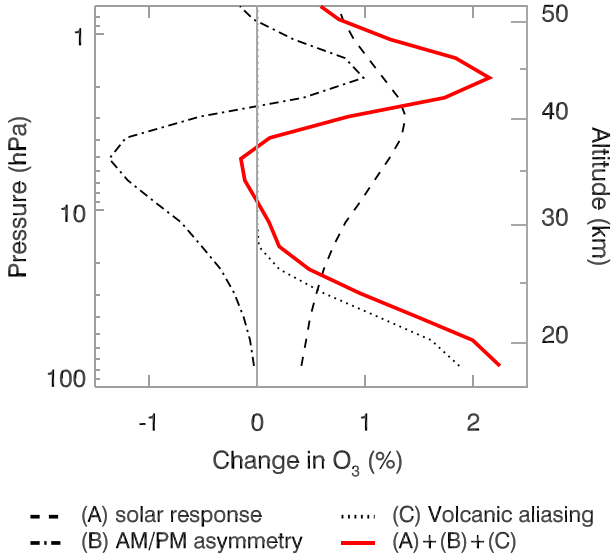

Figure 3. An empirical model that explains the insignificant stratospheric minimum of the 11 year solar cycle response in SBUV O_3. The average solar response (Experiment A; dashed line) is defined as the O_3 deviation for an average $\Delta F_{10.7} = 50$ sfu during 1990–2000. The average diurnal deviation (Experiment B; dash-dotted line) is defined as the O_3 changes from 12 P.M. to 2 P.M. during summer. The aliasing effect due to volcanic eruption (Experiment C) is extracted from Figure 9 of *Chiodo et al.* [2014]. The total effect (red solid line) is the sum of the three vertical profiles.

the orbital drift. The result is shown as the dash-dotted line in Figure 3. It has a positive peak (1.5%/100 $F_{10.7}$) at 2 hPa and a negative peak (−1.2%/100 $F_{10.7}$) at 5 hPa.

However, none of these experiments reproduces the lower stratospheric peak because of the absence of aerosol variability in the 1-D photochemical model. Two of the experiments performed by *Chiodo et al.* [2014] examined the total changes of vertical O_3 due to all forcings (solar, QBO, ENSO, and volcanic eruptions) and the partial changes without volcanic eruptions, showing that the lower stratospheric peak below 30 hPa resulted from the aliasing between the volcanic eruptions and the 11 year solar cycle; see their Figure 9. To add this aliasing effect to our simulated O_3 solar cycle response, we define the O_3 changes below 30 hPa associated with volcanic eruptions as the difference between their "all forcing" run and their "no volcanic forcing" run; above 10 hPa, we assume that the aliasing effect is zero (Experiment C; dotted line in Figure 3).

The sum of the simulated 11 year solar cycle response, the A.M./P.M. diurnal asymmetry of vertical O_3, and the aliasing due to volcanic eruptions is shown as the red line in Figure 3. It exhibits a double-peak structure that closely resembles the O_3 decadal variability observed by SBUV. There is a positive peak (2%/100 $F_{10.7}$) at 2 hPa due to the P.M. surplus. More interestingly, this peak also masks the maximum of the photochemical solar response below at 3 hPa, which would explain the unexpected upward shift of the upper stratospheric peak of the SBUV O_3 response. There is also a nearly zero response in the middle stratosphere, which is due to the cancellation between the P.M. deficit and the photochemical solar response in the middle stratosphere. Thus, these two characteristics of the SBUV double-peak structure that have been previously attributed to the O_3 solar response can be adequately explained in terms of the O_3 A.M./P.M. diurnal asymmetry. The lower stratospheric peak, in contrast, is largely due to the aliasing effect of two volcanic eruptions a decade apart that affected ozone through aerosol-ozone interaction. It is not solar cycle forced.

3.2. Other Satellite Measurements With Minimal Orbital Artifacts

The effects of A.M./P.M. asymmetry on the extracted solar cycle response can be independently verified using other satellite O_3 data that are not subject to large diurnal variability, for example, the O_3 solar response extracted from the observations by the Halogen Occultation Experiment (HALOE) and Stratospheric Aerosol and Gas Experiment (SAGE) II. HALOE and SAGE II are limb scanners, and the abundances of atmospheric tracers can be retrieved along the tangent lines of atmospheric layers that are not limited by the satellite position in the orbit. Therefore, HALOE and SAGE-II measurements provide more data points on the diurnal cycle than SBUV's nadir measurements, so that the effects of the diurnal variations may be minimized in the monthly average of the O_3 profile. Note that, however, these instrument records are rather short, and so the regressed results have large uncertainties. The HALOE and SAGE-II data can be obtained from the Global Ozone Chemistry and Related Trace Gas Data Records for the Stratosphere (GOZCARDS) Project.

The monthly average of the ozone time series is first removed from the data. The solar cycle modulation is retrieved using the following regression model:

$$O_3(t) = \alpha t + \beta F_{10.7}(t) + \gamma_1 \mathrm{QBO}_1(t) + \gamma_2 \mathrm{QBO}_2(t) + \lambda \mathrm{ENSO}(t) + \mu\tau(t) + \text{residual} \quad (1)$$

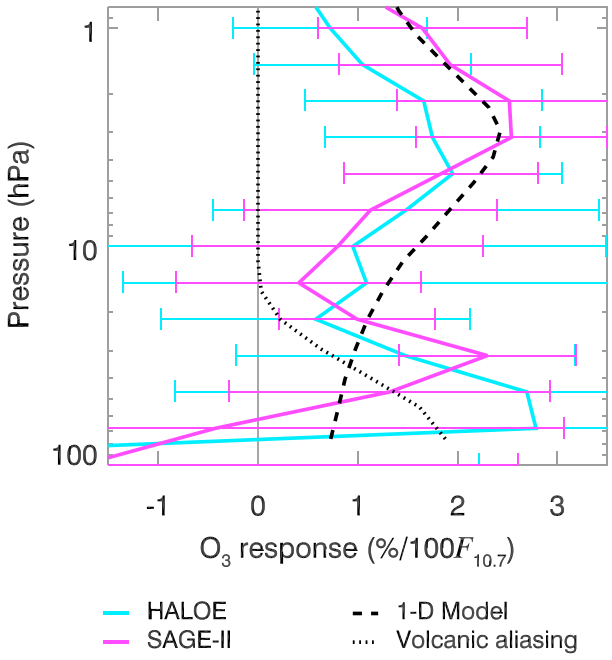

Figure 4. Comparisons of the 11 year solar cycle responses of O_3 obtained from the 1-D eddy-diffusive photochemical model with those obtained from HALOE and SAGE-II O_3 measurements. The volcanic aliasing predicted by *Chiodo et al.* [2014] is also shown.

where αt is a linear trend in time t, $F_{10.7}(t)$ is the 10.7 cm solar radio flux, and $QBO_1(t)$ and $QBO_2(t)$ are a pair of QBO indices derived from stratospheric zonal winds over Singapore [*Wallace et al.*, 1993]. $QBO_1(t)$ is approximately the difference of the zonal winds at 70 hPa and 10 hPa, and $QBO_2(t)$ is approximately the zonal wind at 30 hPa. Using these two indices together could capture the downward propagation of the QBO signal [*Randel and Wu*, 1996; *Li et al.*, 2008]. ENSO(t) is the ENSO index described by the Multivariate ENSO Index [*Wolter and Timlin*, 2011]; $\tau(t)$ is the stratospheric aerosol optical thickness at 550 nm. The coefficients α, β, γ_1, γ_2, λ, and μ are obtained using multiple linear regression.

Figure 4 compares the O_3 solar cycle response in the 1-D photochemical model with those from HALOE, and SAGE II. We note that these measurements also show an upper stratospheric peak of ozone at 3 hPa, consistent with the model prediction. Furthermore, the middle stratospheric responses at 10 hPa observed by these measurements agree with the model prediction much better than that of SBUV. However, the shorter lengths of these satellite observations lead to much larger regression error bars, which preclude a determination of the vertical structure of the solar cycle signal throughout stratosphere.

We note that SAGE-II version 6.2 O_3 mixing ratios are used in the GOZCARDS database, which may result in an overestimated solar cycle response at ~50 km [*Dhomse et al.*, 2016]. However, the agreement between the vertical responses extracted from HALOE and SAGE II in Figure 4 shows that our conclusion is robust.

3.3. Feasibility of Other Proposed Causes of O_3 Decadal Variability

The A.M./P.M. diurnal asymmetry of O_3 induced by the orbital drift is only one of the possible mechanisms that leads to a double-peak structure in the O_3 decadal variability. Other proposed mechanisms have been studied extensively in previous studies. They can be categorized into three premises: missing stratospheric dynamics, incomplete O_3 photochemistry, or uncertainties in photochemical parameters. Below, we review the feasibility of these proposed mechanisms.

3.3.1. Missing Stratospheric Dynamics

Soukharev and Hood [2006] argue that the tropical ascent associated with the secondary circulation of QBO under solar maximum condition might have been reduced, such that odd-nitrogen species (NO_x) would accumulate in the middle stratosphere and catalytically destroy O_3 [*Chipperfield and Gray*, 1992]. However, models fail to simulate any changes of QBO (prescribed or self-generated) due to solar cycle forcing [*McCormack et al.*, 2007; *Smith and Matthes*, 2008; *Schmidt et al.*, 2010; *Dhomse et al.*, 2011; *Chiodo et al.*, 2012; *Matthes et al.*, 2013]. Weakened tropical ascent associated with the Brewer-Dobson circulation resulted from a polar QBO-solar cycle interaction [*Kodera and Kuroda*, 2002; *Kuroda and Kodera*, 2002] may also introduce an accumulation of middle stratospheric NO_x but such polar interaction may not be statistically robust [*Camp and Tung*, 2007; *Li and Tung*, 2014]. Some studies anticipate that the observed middle stratospheric minimum may be a decadal beat due to aliasing between the QBO and the annual cycle, not related to the solar cycle [*Lee and Smith*, 2003]. But this argument works only if the average QBO period is 26–27 months; observationally, the average QBO period is 28 months [*Kuai et al.*, 2009], and the resulting beat frequency (7 years) is significantly different from a decadal signal.

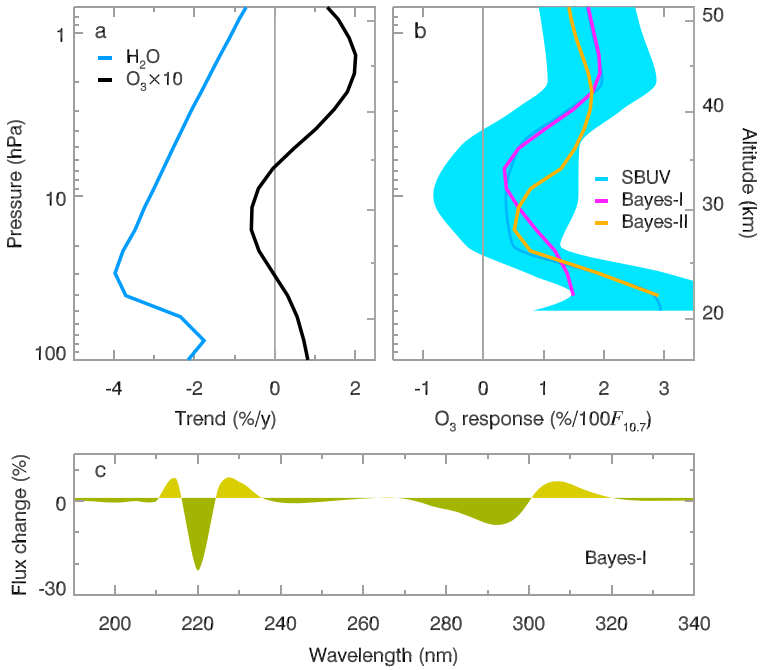

Figure 5. (a) O_3 decadal trend (multiplied by 10; black line) resulting from the trend in stratospheric water vapor (H_2O; blue line). (b) Two Bayesian inversions of model parameters against the decadal variability obtained from SBUV O_3. In the first experiment (Bayes I; magenta line), the solar spectral UV is allowed to vary; in the second experiment (Bayes II; orange line), the chemical kinetic cross sections of the Chapman chemistry are allowed to vary. The SBUV O_3 response is the same as the one shown in Figure 1. (c) The best fitted spectral UV changes after the Bayesian inversion in Experiment Bayes I. Only wavelengths between 190 and 340 nm are shown; changes at other wavelengths are insignificant.

3.3.2. Incomplete Photochemistry

Model simulations suggest that inhomogeneous source of mesospheric NO_x produced at high latitudes by solar electron precipitation during solar maximum may be transported to lower altitudes in tropics to enhance middle stratospheric O_3 destruction [*Callis et al.*, 2001; *Rozanov et al.*, 2005]. However, observed decadal changes of middle stratospheric NO_x, regardless of the source, are too small (~10%) to explain the middle stratospheric minimum [*Hood and Soukharev*, 2006]. It has also been suggested that long-term trends in water vapor (H_2O) and methane (CH_4) may contribute to decadal variability of middle stratospheric O_3 through their conversion to odd-hydrogen species (HO_x) [*Remsberg*, 2010; *Hurst et al.*, 2011; *Hegglin et al.*, 2014]. We test this hypothesis by calculating the O_3 change associated with the H_2O trend using the 1-D photochemical model, assuming that stratospheric CH_4 is ultimately photolyzed to H_2O. At 30 km, the decrease in O_3 is −0.5% per decade only, which is again too small to explain the middle stratospheric minimum (Figure 5a).

3.3.3. Uncertainties in Photochemical Parameters

Previous studies have considered two types of uncertainties: measurement uncertainties in the solar spectral UV [*Ermolli et al.*, 2013] and laboratory uncertainties in the chemical kinetic cross section [*Sander et al.*, 2011]. Current long-term records of the solar spectral UV merged from various data sets may be subject to large decadal uncertainty due to different instrument calibrations and sensitivities, which may impact O_3 simulation significantly [*Haigh et al.*, 2010; *Ball et al.*, 2014a, 2016]. Here we examine whether the observed double-peak O_3 solar cycle response is consistent with the aforementioned uncertainties. Using a Bayesian inversion [*Rodgers*, 2000; *Ball et al.*, 2014b], we vary the UV intensity in the 1-D model to fit the observed 11 year solar cycle response in O_3, assuming 20% uncertainty in UV variability between 110–350 nm related to the solar cycle and 5–10% uncertainty in the observed O_3 solar response (Experiment "Bayes I"). Although the model has no interactive dynamics, we can reproduce a double-peak O_3 solar response (Figure 5b; magenta line) by reducing the UV variation near 220 nm by 20% and 290 nm by 10% and increasing the UV variation near 305 nm by 10% (Figure 5c). The reduction of UV variation at 220 nm is equivalent to a reduction in O_2 photolysis rate. We perform another Bayesian inversion assuming 20% uncertainty in the chemical kinetic cross

Table 1. Results of Experiment "Bayes II," in Which the Chemical Kinetic Cross Sections of the Chapman Chemistry Are Allowed to Vary[a]

Photochemical Reactions	Changes in Chemical Kinetic Cross Sections
O_2 + photon (≤240 nm) → O + O	+30%
O_3 + photon (200–360 nm) → O_2 + O	−30%
O + O_3 → O_2 + O_2	−30%

[a]Only the three most significant reactions are listed.

sections associated with the Chapman reactions (Experiment "Bayes II"). A double-peak O_3 solar response can also be reproduced (Figure 5b; orange line) by increasing O_2 photolysis rate by 30% and by reducing both O_3 photolysis rate and O + O_3 recombination rate by 30% (Table 1). Thus, both Bayesian inversions may lead to an O_3 solar response that is consistent with the SBUV observations, but the inferred changes of O_2 photolysis rates of opposite signs. We argue that simply assuming uncertainties in model parameters offers too many degrees of freedom and generally do not provide unique solutions to model deficiencies, obscuring physical interpretations.

4. Conclusions

We have revisited a persistent model-observation discrepancy of the 11 year solar cycle response in tropical stratospheric O_3: while standard photochemical models predict a single-peak response in the stratosphere, satellite observations show an unexpected double-peak structure. This discrepancy has led to the question of whether the current standard O_3 photochemistry is deficient. We have shown that the decadal satellite orbital drifts relative to the diurnal cycle may be a cause of the discrepancy. Our photochemical model is capable of explaining two important features of the 11 year solar cycle response in O_3 observed by SBUV: (1) The P.M. O_3 surplus at 2 hPa dominates over the O_3 photochemical solar response at 3 hPa, leading to an unexpected upward shift of the O_3 decadal variability that has been previously thought to be a solar-induced feature, and (2) the cancellation between the P.M. deficit and the photochemical solar response in the middle stratosphere leads to a near-zero response that has been previously thought to be due to nonlinear dynamics and heterogeneous chemistry. Besides the A.M./P.M. diurnal asymmetry, we have also discussed some important aspects and shortcomings of other possible mechanisms proposed in previous studies to explain the double-peak structure in the observed O_3 decadal variability by SBUV.

With the A.M./P.M. diurnal asymmetry of O_3 taken into consideration, we assert that the standard photochemistry is consistent with the observed solar cycle modulation in stratospheric O_3. Thus, the ozone decadal variability driven by the 11 year solar cycle provides a robust test for chemistry/climate models.

Acknowledgments
K.F.L. thanks William J. Randel and Lucien Froidevaux for an illuminating discussion. We thank Irene Chen, Mimi Gerstell, Run-Lie Shia, Sally Newman, Pushkar Kopparla, and Stanley P. Sander for reading the manuscript. K.F.L. has been partially supported by the NASA Jack Eddy Fellowship administrated by the University Corporation for Atmospheric Research. K.F.L. and K.K.T. have been supported by the NASA grant NNX14AR40G. Q.Z. and Y.L.Y. acknowledge partial support by NASA's LWS program via grant NNX16AK63G to the California Institute of Technology. The GOZCARDS data were obtained from https://gozcards.jpl.nasa.gov/. The SAGE-corrected SBUV data can be obtained from ftp://es-ee.tor.ec.gc.ca/pub/SAGE_corrected_SBUV/. The 10.7 cm solar radio flux was obtained from http://www.spaceweather.ca/. The stratospheric zonal winds for deriving the two QBO indices were obtained from http://www.geo.fu-berlin.de/en/met/ag/strat/produkte/qbo/qbo.dat. The Multivariate ENSO index was obtained from http://www.esrl.noaa.gov/psd/enso/mei.ext. The stratospheric aerosol optical thickness at 550 nm was obtained from http://data.giss.nasa.gov/modelforce/strataer/. The SORCE solar spectral data can be obtained from http://lasp.colorado.edu/home/sorce/data/.

References

Allen, M., Y. L. Yung, and J. W. Waters (1981), Vertical transport and photochemistry in the terrestrial mesosphere and lower thermosphere (50–120 km), *J. Geophys. Res.*, *86*, 3617–3627, doi:10.1029/JA086iA05p03617.

Allen, M., J. I. Lunine, and Y. L. Yung (1984), The vertical-distribution of ozone in the mesosphere and lower thermosphere, *J. Geophys. Res.*, *89*, 4841–4872, doi:10.1029/JD089iD03p04841.

Austin, J., et al. (2008), Coupled chemistry climate model simulations of the solar cycle in ozone and temperature, *J. Geophys. Res.*, *113*, D11306, doi:10.1029/2007JD009391.

Ball, W. T., N. A. Krivova, Y. C. Unruh, J. D. Haigh, and S. K. Solanki (2014a), A new SATIRE-S spectral solar irradiance reconstruction for solar cycles 21–23 and its implications for stratospheric ozone, *J. Atmos. Sci.*, *71*, 4086–4101, doi:10.1175/JAS-D-13-0241.1.

Ball, W. T., D. J. Mortlock, J. S. Egerton, and J. D. Haigh (2014b), Assessing the relationship between spectral solar irradiance and stratospheric ozone using Bayesian inference, *J. Space Weather Space Clim.*, *4*, A25, doi:10.1051/swsc/2014023.

Ball, W. T., J. D. Haigh, E. V. Rozanov, A. Kuchar, T. Sukhodolov, F. Tummon, A. V. Shapiro, and W. Schmutz (2016), High solar cycle spectral variations inconsistent with stratospheric ozone observations, *Nat. Geosci.*, *9*, 206–209, doi:10.1038/ngeo2640.

Bates, D. R., and M. Nicolet (1950), The photochemistry of atmospheric water vapor, *J. Geophys. Res.*, *55*, 301–327, doi:10.1029/JZ055i003p00301.

Bhartia, P. K., R. D. McPeters, L. E. Flynn, S. Taylor, N. A. Kramarova, S. Frith, B. Fisher, and M. DeLand (2013), Solar backscatter UV (SBUV) total ozone and profile algorithm, *Atmos. Meas. Tech.*, *6*, 2533–2548, doi:10.5194/amt-6-2533-2013.

Brasseur, G., and S. Solomon (2005), *Aeronomy of the Middle Atmosphere: Chemistry and Physics of the Stratosphere and Mesosphere*, 3rd ed., Springer, Dordrecht, Neth.

Brasseur, G., M. H. Hitchman, P. C. Simon, and A. Derudder (1988), Ozone reduction in the 1980s: A model simulation of anthropogenic and solar perturbations, *Geophys. Res. Lett.*, *15*, 1361–1364, doi:10.1029/GL015i012p01361.

Brewer, A. W. (1949), Evidence for a world circulation provided by measurements of helium and water vapour distribution in the stratosphere, *Q. J. R. Meteorol. Soc.*, *75*, 351–363, doi:10.1002/qj.49707532603.
Callis, L. B., M. Natarajan, and J. D. Lambeth (2001), Solar-atmospheric coupling by electrons (SOLACE): 3. Comparisons of simulations and observations, 1979–1997, issues and implications, *J. Geophys. Res.*, *106*, 7523–7539, doi:10.1029/2000JD900615.
Camp, C. D., and K.-K. Tung (2007), The influence of the solar cycle and QBO on the late-winter stratospheric polar vortex, *J. Atmos. Sci.*, *64*, 1267–1283, doi:10.1175/JAS3883.1.
Chapman, S. (1930), On ozone and atomic oxygen in the upper atmosphere, *Philos. Mag.*, *10*, 369–383.
Chiodo, G., N. Calvo, D. R. Marsh, and R. Garcia-Herrera (2012), The 11 year solar cycle signal in transient simulations from the Whole Atmosphere Community Climate Model, *J. Geophys. Res.*, *117*, D06109, doi:10.1029/2011JD016393.
Chiodo, G., D. R. Marsh, R. Garcia-Herrera, N. Calvo, and J. A. Garcia (2014), On the detection of the solar signal in the tropical stratosphere, *Atmos. Chem. Phys.*, *14*, 5251–5269, doi:10.5194/acp-14-5251-2014.
Chipperfield, M. P., and L. J. Gray (1992), Two-dimensional model studies of the interannual variability of trace gases in the middle atmosphere, *J. Geophys. Res.*, *97*, 5963–5980, doi:10.1029/92JD00029.
Crutzen, P. J. (1970), Influence of nitrogen oxides on atmospheric ozone content, *Q. J. R. Meteorol. Soc.*, *96*, 320–325, doi:10.1002/qj.49709640815.
DeLand, M. T., S. L. Taylor, L. K. Huang, and B. L. Fisher (2012), Calibration of the SBUV version 8.6 ozone data product, *Atmos. Meas. Tech.*, *5*, 2951–2967, doi:10.5194/amt-5-2951-2012.
Dhomse, S. S., M. P. Chipperfield, W. Feng, and J. D. Haigh (2011), Solar response in tropical stratospheric ozone: A 3-D chemical transport model study using ERA reanalyses, *Atmos. Chem. Phys.*, *11*, 12773–12786, doi:10.5194/acp-11-12773-2011.
Dhomse, S. S., M. P. Chipperfield, W. Feng, R. Hossaini, G. W. Mann, and M. L. Santee (2015), Revisiting the hemispheric asymmetry in midlatitude ozone changes following the Mount Pinatubo eruption: A 3-D model study, *Geophys. Res. Lett.*, *42*, 3038–3047, doi:10.1002/2015GL063052.
Dhomse, S. S., M. P. Chipperfield, R. P. Damadeo, J. M. Zawodny, W. T. Ball, W. Feng, R. Hossaini, G. W. Mann, and J. D. Haigh (2016), On the ambiguous nature of the 11 year solar cycle signal in upper stratospheric ozone, *Geophys. Res. Lett.*, *43*, 7241–7249, doi:10.1002/2016GL069958.
Dobson, G. M. B. (1956), Origin and distribution of polyatomic molecules in the atmosphere, *Proc. R. Soc. A*, *236*, 187–193, doi:10.1098/rspa.1956.0127.
Ermolli, I., et al. (2013), Recent variability of the solar spectral irradiance and its impact on climate modelling, *Atmos. Chem. Phys.*, *13*, 3945–3977, doi:10.5194/acp-13-3945-2013.
Farman, J. C., B. G. Gardiner, and J. D. Shanklin (1985), Large losses of total ozone in Antarctica reveal seasonal ClO_x/NO_x interaction, *Nature*, *315*, 207–210, doi:10.1038/315207a0.
Forster, P. M. D., and K. P. Shine (1997), Radiative forcing and temperature trends from stratospheric ozone changes, *J. Geophys. Res.*, *102*, 10,841–10,855, doi:10.1029/96JD03510.
Haefele, A., K. Hocke, N. Kampfer, P. Keckhut, M. Marchand, S. Bekki, B. Morel, T. Egorova, and E. Rozanov (2008), Diurnal changes in middle atmospheric H_2O and O_3: Observations in the Alpine region and climate models, *J. Geophys. Res.*, *113*, D17303, doi:10.1029/2008JD009892.
Haigh, J. D., A. R. Winning, R. Toumi, and J. W. Harder (2010), An influence of solar spectral variations on radiative forcing of climate, *Nature*, *467*, 696–699, doi:10.1038/nature09426.
Hegglin, M. I., et al. (2014), Vertical structure of stratospheric water vapour trends derived from merged satellite data, *Nat. Geosci.*, *7*, 768–776, doi:10.1038/ngeo2236.
Hood, L. L., and B. E. Soukharev (2006), Solar induced variations of odd nitrogen: Multiple regression analysis of UARS HALOE data, *Geophys. Res. Lett.*, *33*, L22805, doi:10.1029/2006GL028122.
Hood, L. L., and B. E. Soukharev (2012), The lower-stratospheric response to 11-Yr solar forcing: Coupling to the troposphere–ocean response, *J. Atmos. Sci.*, *69*, 1841–1864, doi:10.1175/JAS-D-11-086.1.
Hood, L. L., J. L. Jirikowic, and J. P. McCormack (1993), Quasi-decadal variability of the stratosphere: Influence of long-term solar ultraviolet variations, *J. Atmos. Sci.*, *50*, 3941–3958, doi:10.1175/1520-0469(1993)050<3941:QDVOTS>2.0.CO;2.
Hurst, D. F., S. J. Oltmans, H. Vomel, K. H. Rosenlof, S. M. Davis, E. A. Ray, E. G. Hall, and A. F. Jordan (2011), Stratospheric water vapor trends over Boulder, Colorado: Analysis of the 30 year Boulder record, *J. Geophys. Res.*, *116*, D02306, doi:10.1029/2010JD015065.
Kodera, K., and Y. Kuroda (2002), Dynamical response to the solar cycle, *J. Geophys. Res.*, *107*(D24), 4749, doi:10.1029/2002JD002224.
Kuai, L., R.-L. Shia, X. Jiang, K. K. Tung, and Y. L. Yung (2009), Nonstationary synchronization of equatorial QBO with SAO in observations and a model, *J. Atmos. Sci.*, *66*, 1654–1664, doi:10.1175/2008JAS2857.1.
Kuroda, Y., and K. Kodera (2002), Effect of solar activity on the polar-night jet oscillation in the Northern and Southern Hemisphere winter, *J. Meteorol. Soc. Jpn.*, *80*, 973–984, doi:10.2151/jmsj.80.973.
Lean, J. (2000), Evolution of the Sun's spectral irradiance since the Maunder Minimum, *Geophys. Res. Lett.*, *27*, 2425–2428, doi:10.1029/2000GL000043.
Lee, H., and A. K. Smith (2003), Simulation of the combined effects of solar cycle, quasi-biennial oscillation, and volcanic forcing on stratospheric ozone changes in recent decades, *J. Geophys. Res.*, *108*(D2), 4049, doi:10.1029/2001JD001503.
Li, K.-F., and K.-K. Tung (2014), Quasi-biennial oscillation and solar cycle influences on winter Arctic total ozone, *J. Geophys. Res.*, *119*, 5823–5835, doi:10.1002/2013JD021065.
Li, T., T. Leblanc, and I. S. McDermid (2008), Interannual variations of middle atmospheric temperature as measured by the JPL lidar at Mauna Loa Observatory, Hawaii (19.5 degrees N, 155.6 degrees W), *J. Geophys. Res.*, *113*, D14109, doi:10.1029/2007JD009764.
Marsh, D. R., and R. R. Garcia (2007), Attribution of decadal variability in lower-stratospheric tropical ozone, *Geophys. Res. Lett.*, *34*, L21807, doi:10.1029/2007GL030935.
Matthes, K., K. Kodera, R. R. Garcia, Y. Kuroda, D. R. Marsh, and K. Labitzke (2013), The importance of time-varying forcing for QBO modulation of the atmospheric 11 year solar cycle signal, *J. Geophys. Res.*, *118*, 4435–4447, doi:10.1002/jgrd.50424.
McCormack, J. P., D. E. Siskind, and L. L. Hood (2007), Solar-QBO interaction and its impact on stratospheric ozone in a zonally averaged photochemical transport model of the middle atmosphere, *J. Geophys. Res.*, *112*, D16109, doi:10.1029/2006JD008369.
McElroy, M. B., R. J. Salawitch, S. C. Wofsy, and J. A. Logan (1986), Reductions of Antarctic ozone due to synergistic interactions of chlorine and bromine, *Nature*, *321*, 759–762, doi:10.1038/321759a0.
Molina, L. T., and M. J. Molina (1987), Production of Cl_2O_2 from the self-reaction of the ClO radical, *J. Phys. Chem.*, *91*, 433–436, doi:10.1021/J100286a035.

Myhre, G., et al. (2013), Anthropogenic and natural radiative forcing, in *Climate Change 2013: The Physical Science Basis. Contribution of Working Group I to the Fifth Assessment Report of the Intergovernmental Panel on Climate Change*, edited by T. F. Stocker et al., pp. 659–740, Cambridge Univ. Press, Cambridge, U. K. and New York.

Randel, W. J., and F. Wu (1996), Isolation of the ozone QBO in SAGE II data by singular-value decomposition, *J. Atmos. Sci.*, *53*, 2546–2559.

Remsberg, E. (2010), Observed seasonal to decadal scale responses in mesospheric water vapor, *J. Geophys. Res.*, *115*, D06306, doi:10.1029/2009JD012904.

Rodgers, C. D. (2000), *Inverse Methods for Atmospheric Sounding: Theory and Practice*, 240 pp., World Sci. Publishing, Singapore.

Rozanov, E., L. Callis, M. Schlesinger, F. Yang, N. Andronova, and V. Zubov (2005), Atmospheric response to NO_y source due to energetic electron precipitation, *Geophys. Res. Lett.*, *32*, L14811, doi:10.1029/2005GL023041.

Sander, S. P., R. R. Friedl, and Y. L. Yung (1989), Rate of formation of the ClO dimer in the polar stratosphere: Implications for ozone loss, *Science*, *245*, 1095–1098, doi:10.1126/science.245.4922.1095.

Sander, S. P., et al. (2006), Chemical kinetics and photochemical data for use in atmospheric studies, Evaluation no. 15, JPL Publication 06–2, Jet Propulsion Laboratory, Pasadena.

Sander, S. P., et al. (2011), Chemical kinetics and photochemical data for use in atmospheric studies, Evaluation no. 17, 684 pp., JPL Publication 10–6, Jet Propulsion Laboratory, Pasadena. [Available at http://jpldataeval.jpl.nasa.gov/.]

Schmidt, H., G. P. Brasseur, and M. A. Giorgetta (2010), Solar cycle signal in a general circulation and chemistry model with internally generated quasi-biennial oscillation, *J. Geophys. Res.*, *115*, D00I14, doi:10.1029/2009JD012542.

Smith, A. K., and K. Matthes (2008), Decadal-scale periodicities in the stratosphere associated with the solar cycle and the QBO, *J. Geophys. Res.*, *113*, D05311, doi:10.1029/2007JD009051.

Solanki, S. K., N. A. Krivova, and J. D. Haigh (2013), Solar irradiance variability and climate, *Ann. Rev. Astron. Astrophys.*, *51*, 311–351, doi:10.1146/annurev-astro-082812-141007.

Solomon, S., R. R. Garcia, F. S. Rowland, and D. J. Wuebbles (1986), On the depletion of Antarctic ozone, *Nature*, *321*, 755–758, doi:10.1038/321755a0.

Soukharev, B. E., and L. L. Hood (2006), Solar cycle variation of stratospheric ozone: Multiple regression analysis of long-term satellite data sets and comparisons with models, *J. Geophys. Res.*, *111*, D20314, doi:10.1029/2006JD007107.

Tung, K.-K., M. K. W. Ko, J. M. Rodriguez, and N. D. Sze (1986), Are antarctic ozone variations a manifestation of dynamics or chemistry, *Nature*, *322*, 811–814, doi:10.1038/322811a0.

Wallace, J. M., R. L. Panetta, and J. Estberg (1993), Representation of the equatorial stratospheric quasi-biennial oscillation in EOF phase space, *J. Atmos. Sci.*, *50*, 1751–1762.

Wang, S., et al. (2013), Midlatitude atmospheric OH response to the most recent 11-y solar cycle, *Proc. Natl. Acad. Sci. U. S. A.*, *110*, 2023–2028, doi:10.1073/pnas.1117790110.

Willett, H. C. (1962), The relationship of total atmospheric ozone to the sunspot cycle, *J. Geophys. Res.*, *67*, 661–670, doi:10.1029/JZ067i002p00661.

Wolter, K., and M. S. Timlin (2011), El Niño/Southern Oscillation behaviour since 1871 as diagnosed in an extended multivariate ENSO index (MEI.ext), *Intl. J. Climatol.*, *31*, 1074–1087, doi:10.1002/joc.2336.

Yung, Y. L., and W. B. DeMore (1999), *Photochemistry of Planetary Atmospheres*, Oxford Univ. Press, New York.

Yung, Y. L., J. P. Pinto, R. T. Watson, and S. P. Sander (1980), Atmospheric bromine and ozone perturbations in the lower stratosphere, *J. Atmos. Sci.*, *37*, 339–353, doi:10.1175/1520-0469(1980)037<0339:ABAOPI>2.0.CO;2.